

**Supplementary information for "Computational screening of transition-metal atom
embedding in 1T-TaS₂ monolayer defects as efficient
oxygen-reduction/evolution-reaction bifunctional catalysts."**

Junkai Xu¹, Xiaoxue Yu¹, Yuebo Gao¹, Yunhao Wang¹, Jianjun

Fang^{1,*}, Jing Li^{1,†}, Xianfang Yue^{2,‡} and A. J. C. Varandas^{1,3,4§}

¹*School of Physics and Physical Engineering, Qufu Normal University, Qufu, Shandong 273165, China*

²*Department of Physics and Information Engineering, Jining University, Qufu 273155, China*

³*Department of Physics, Universidade Federal do Espírito Santo, 29075-910 Vitória, Brazil and*

⁴*Department of Chemistry and Coimbra Chemistry Centre,
University of Coimbra, 3004-535 Coimbra, Portugal*

(Dated: May 12, 2025)

PACS numbers:

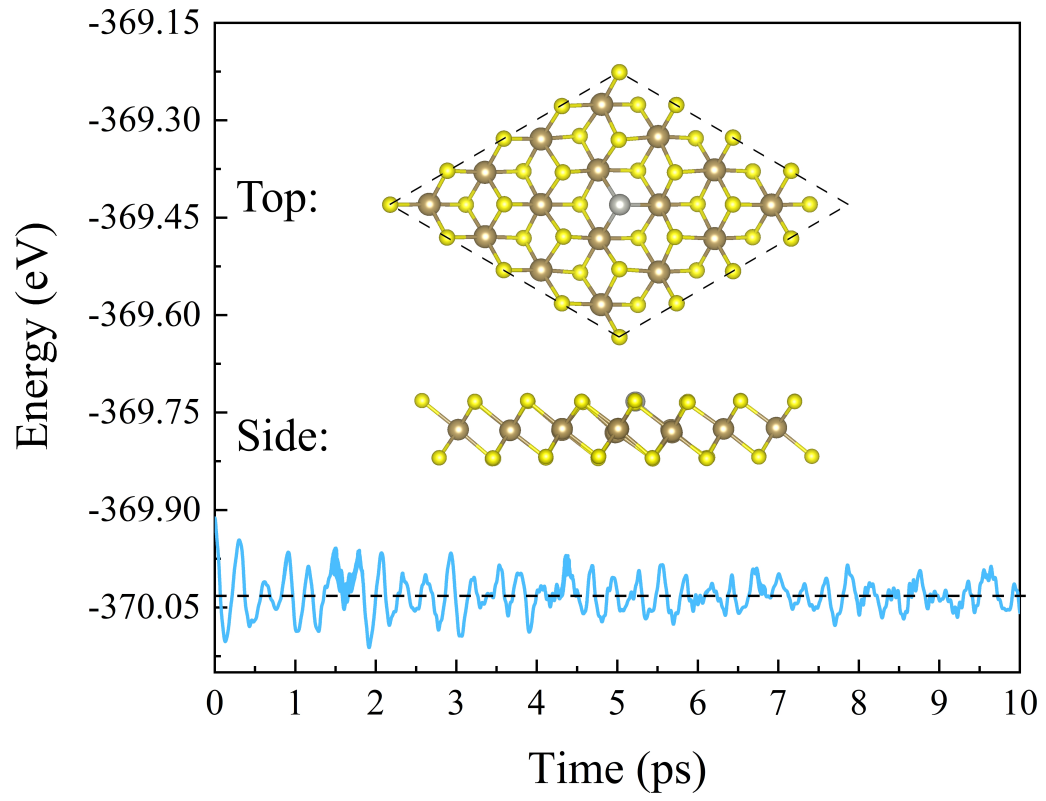


FIG. S1: AIMD simulations of Pd@1T-TaS₂ at 500 K with insets corresponding to the final state structures.

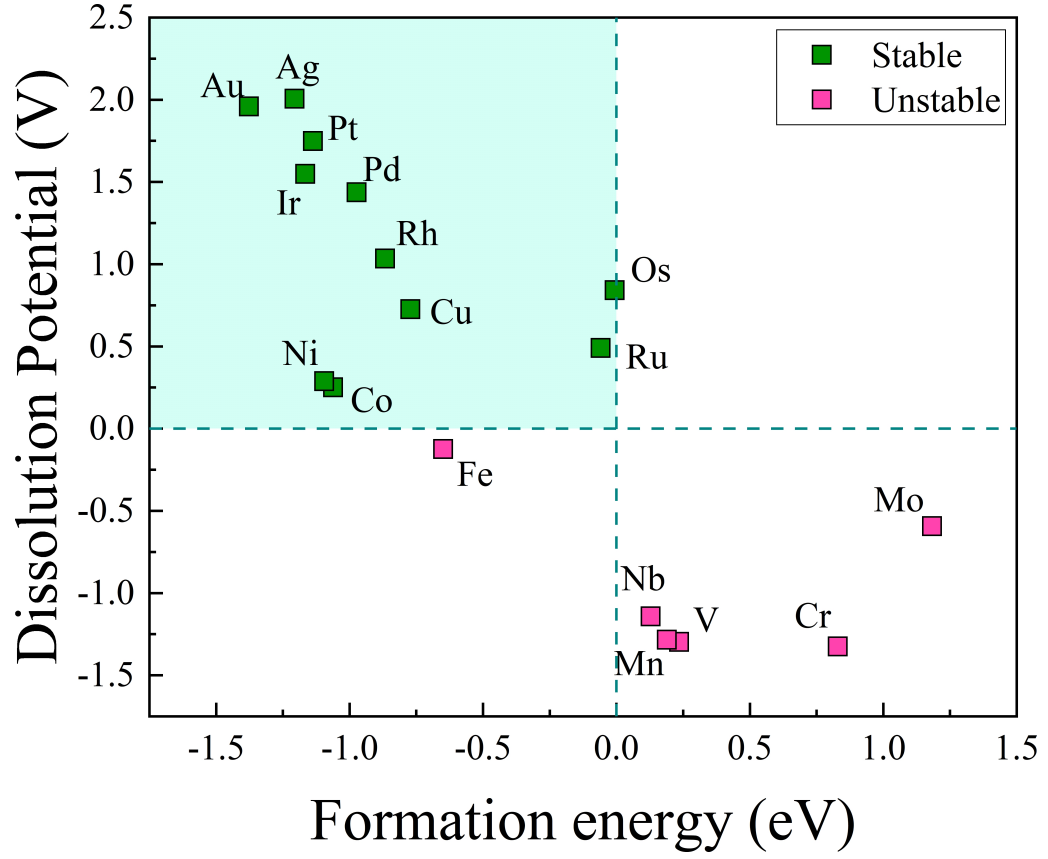


FIG. S2: Formation energy (E_{form}) and dissolution potential (U_{diss}) of TM atoms on TM@1T-TaS₂.

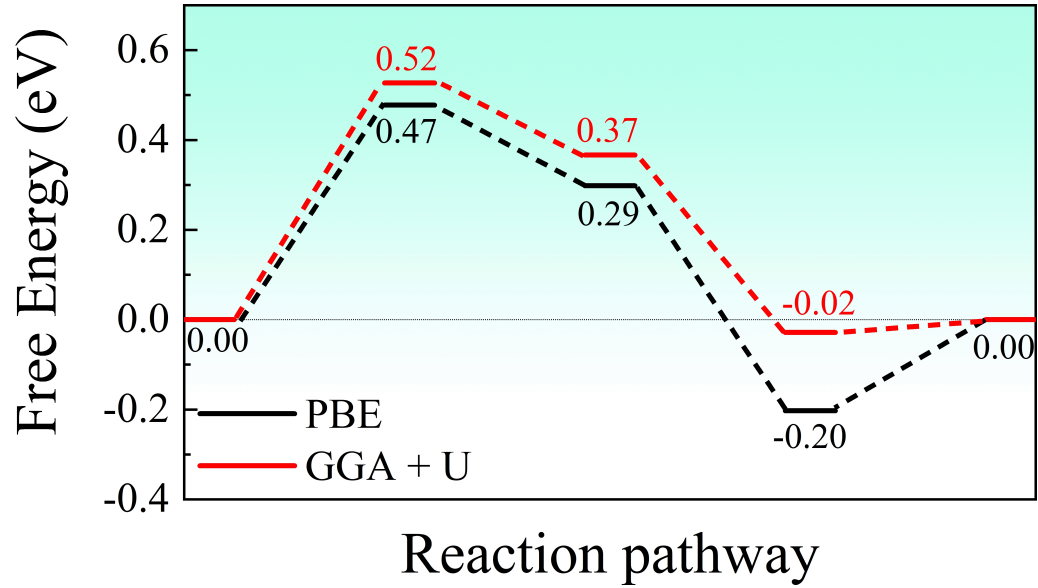


FIG. S3: Free energy change diagram for four-electron transfers on Pd@1T-TaS₂, the red line represents the GGA + U method and the black line represents the PBE method.

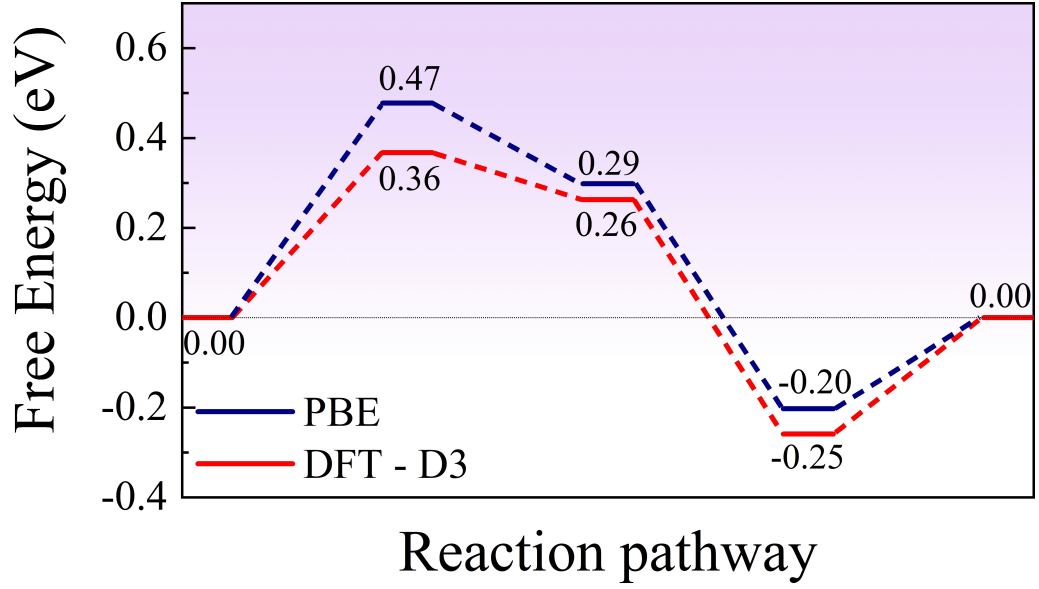


FIG. S4: Free energy change diagram for four-electron transfers on Pd@1T-TaS₂, the red line represents the DFT - D3 method and the navy blue line represents the PBE method.

TABLE S1: The computed E_{bind} , E_{coh} , E_{form}

	E_{bind}	E_{coh}	E_{form}
V@1T-TaS ₂	-5.07	-5.31	0.23
Cr@1T-TaS ₂	-3.27	-4.10	0.82
Mn@1T-TaS ₂	-2.73	-2.92	0.18
Fe@1T-TaS ₂	-4.92	-4.28	-0.64
Co@1T-TaS ₂	-5.45	-4.39	-1.06
Ni@1T-TaS ₂	-5.53	-4.44	-1.09
Cu@1T-TaS ₂	-4.26	-3.49	-0.77
Nb@1T-TaS ₂	-7.44	-7.57	0.12
Mo@1T-TaS ₂	-5.63	-6.82	1.18
Ru@1T-TaS ₂	-6.79	-6.74	-0.05
Rh@1T-TaS ₂	-6.61	-5.75	-0.86
Pd@1T-TaS ₂	-4.86	-3.89	-0.97
Ag@1T-TaS ₂	-4.15	-2.95	-1.20
Os@1T-TaS ₂	-8.17	-8.17	-0.01
Ir@1T-TaS ₂	-8.10	-6.94	-1.16
Pt@1T-TaS ₂	-6.97	-5.84	-1.13
Au@1T-TaS ₂	-5.18	-3.81	-1.37

of TM@1T-TaS₂.

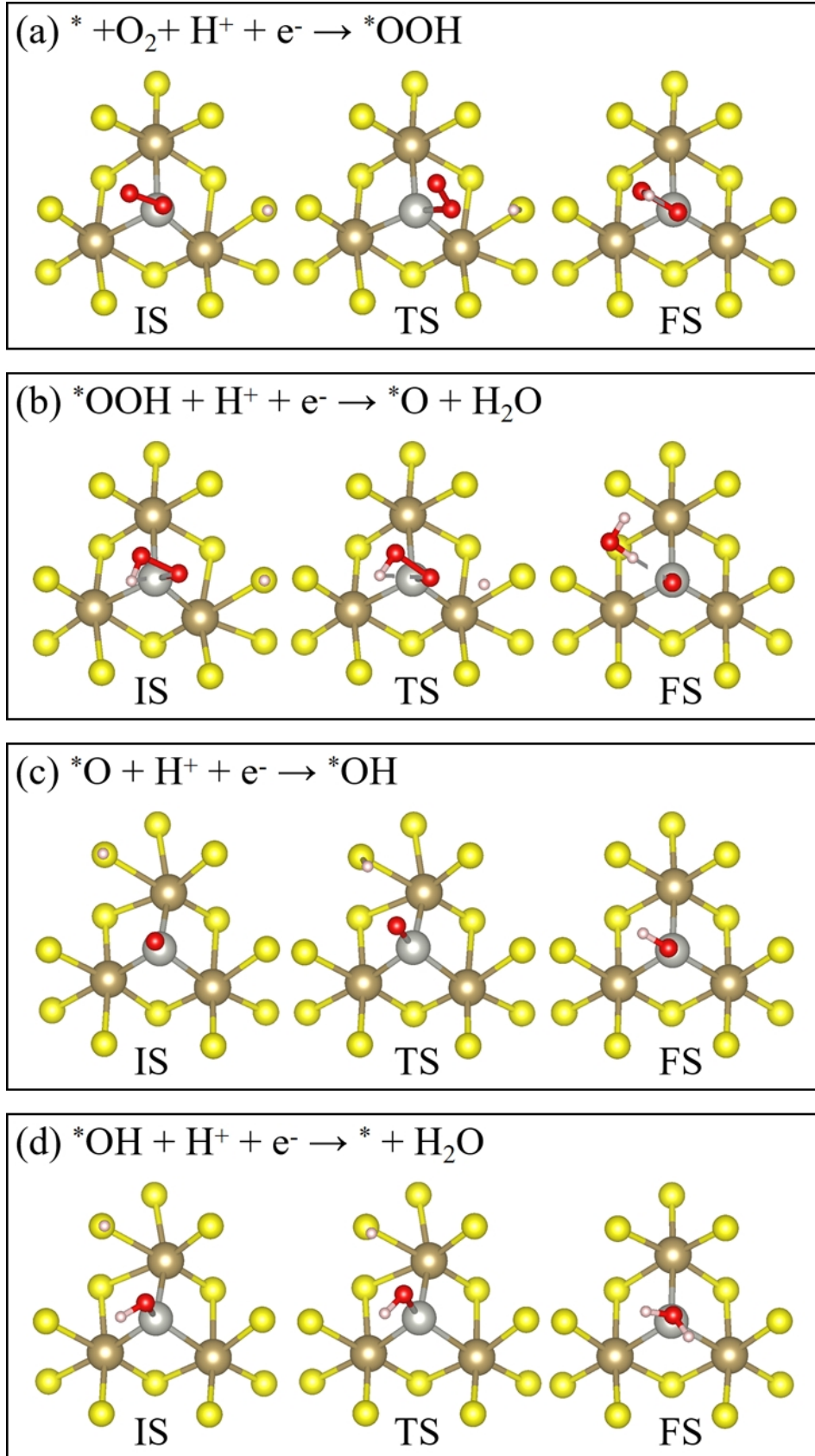


FIG. S5: Structure of the initial, final and transition states involved in the four-electron transfer process on Pd@1-TaS₂: (a) $* + \text{O}_2 + \text{H}^+ + \text{e}^- \rightarrow *\text{OOH}$, (b) $*\text{OOH} + \text{H}^+ + \text{e}^- \rightarrow *\text{O} + \text{H}_2\text{O}$, (c) $*\text{O} + \text{H}^+ + \text{e}^- \rightarrow *\text{OH}$, (d) $*\text{OH} + \text{H}^+ + \text{e}^- \rightarrow * + \text{H}_2\text{O}$.

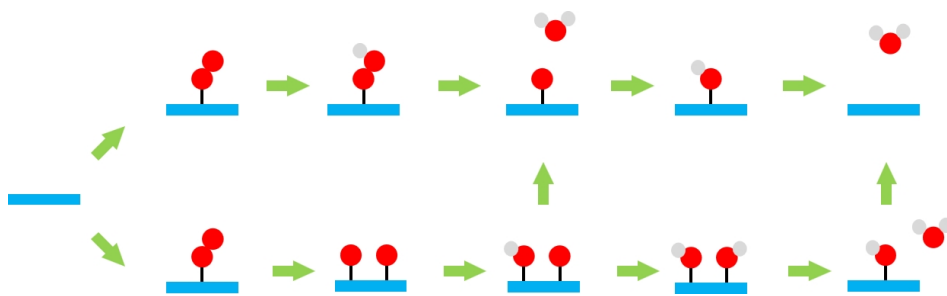


FIG. S6: Association and dissociation pathways of O₂ on catalysts.

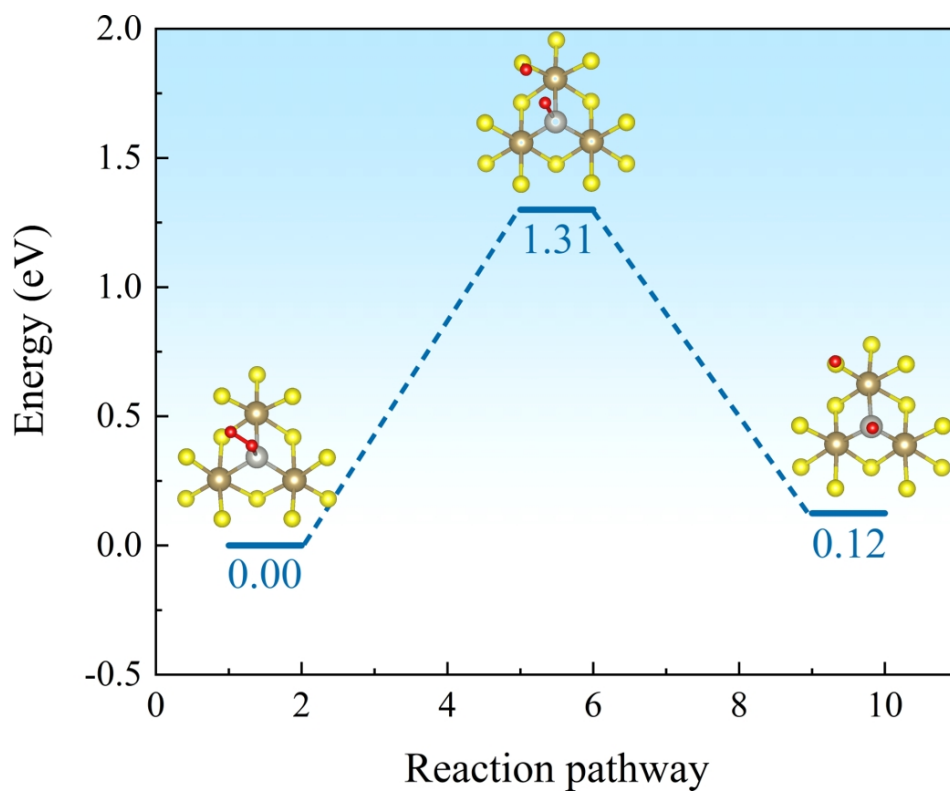


FIG. S7: Energy barrier for O₂ dissociation on Pd@1T-TaS₂, with insets corresponding to the corresponding structures.

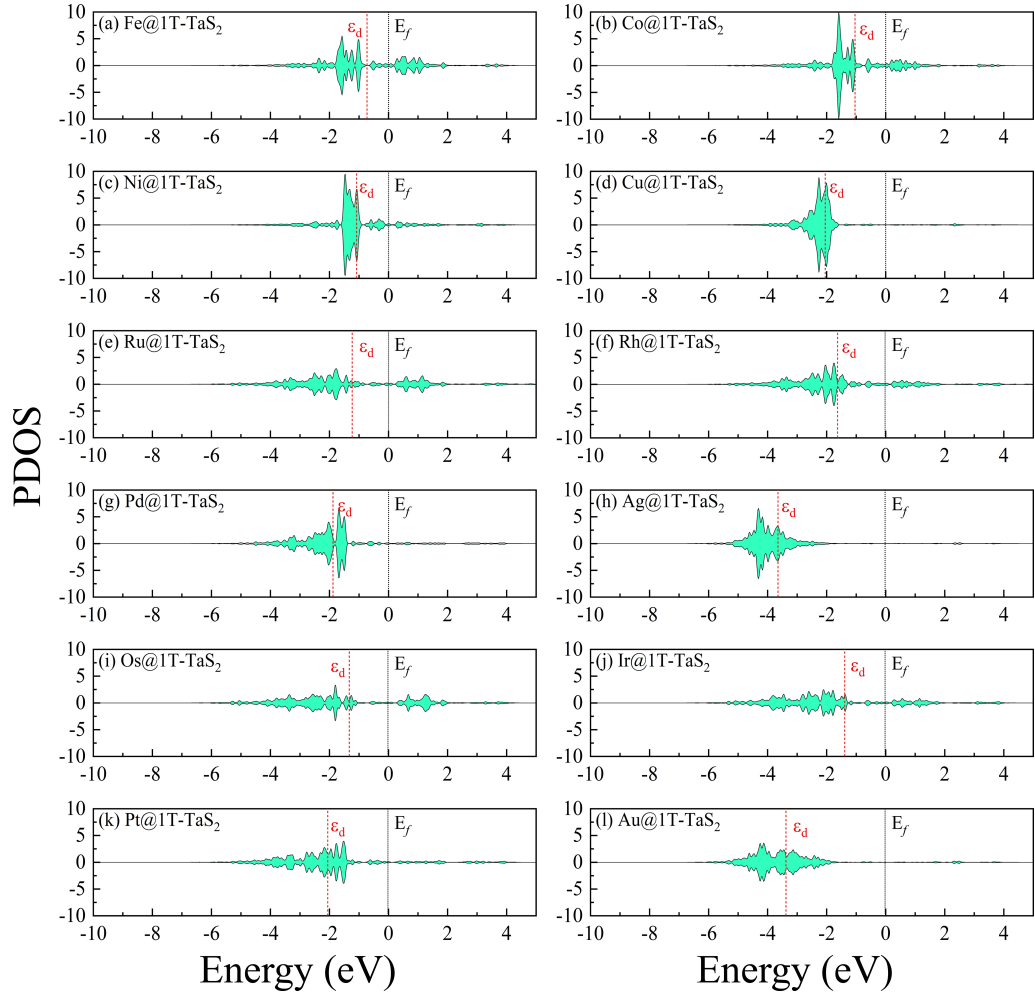


FIG. S8: Partial density of states (PDOS) of d orbitals for TM@1T-TaS₂, the d-band centers (ϵ_d) are marked by red dashed, and the Fermi level (E_f) are set to 0 eV.

TABLE S2: The computed adsorption energy of $^*\text{OH}$, $^*\text{O}$, $^*\text{OOH}$ of TM@1T-TaS₂.

	$\Delta G_{^*\text{OH}}$	$\Delta G_{^*\text{O}}$	$\Delta G_{^*\text{OOH}}$
Fe@1T-TaS ₂	-0.24	0.83	3.06
Co@1T-TaS ₂	-0.18	0.92	3.10
Ni@1T-TaS ₂	0.20	1.78	3.55
Cu@1T-TaS ₂	0.76	3.01	4.03
Ru@1T-TaS ₂	0.00	1.11	3.21
Rh@1T-TaS ₂	0.26	1.53	3.46
Pd@1T-TaS ₂	1.04	2.77	4.18
Ag@1T-TaS ₂	1.44	4.03	4.61
Os@1T-TaS ₂	-0.41	0.60	2.84
Ir@1T-TaS ₂	-0.27	0.71	3.00
Pt@1T-TaS ₂	0.75	1.84	4.08
Au@1T-TaS ₂	1.30	3.37	4.51